



# Tracing Galactic dust kinematics with the diffuse interstellar bands

G. Zasowski \*

Johns Hopkins University 3400 N Charles St Baltimore, MD 21218, USA  
e-mail: gail.zasowski@gmail.com

**Abstract.** The density, chemistry, and circulation of a galaxy's interstellar medium (ISM) has an enormous impact on the chemical evolution of its stars. Understanding this impact requires a complete picture of this phase space for all ISM components, as well as their interactions with each other. In this proceeding, we focus on two ISM components: carbon-rich large molecules, whose distribution and kinematics on galactic scales remains relatively unknown, and dust, whose kinematics have not been measured with standard dust measurement techniques. To trace the former, we turn to the set of interstellar absorption features known as the diffuse interstellar bands (DIBs). In particular, the strongest infrared DIB (at  $1.5272\mu\text{m}$ ) has been used to characterize the large-scale distribution and properties of the Galactic ISM, including in the heavily reddened bulge and inner disc. This DIB absorption's tight correlation with foreground reddening makes it a powerful, independent probe of line-of-sight dust extinction. Here, we use this correlation to, for the first time, assign velocities to individual interstellar clouds of dust and carbon-rich molecules. This is a critical advance along the way to a comprehensive multi-dimensional mapping of the complex ISM system. In the near future, surveys including *Gaia* will produce measurements of a variety of DIB absorption features, along with high quality stellar distances, for a sample of sight-lines numbering in the millions. These datasets will enable unprecedented characterization of the ISM's phase distribution, velocity field, and component correlations.

## 1. Introduction

The interstellar medium (ISM) of a galaxy plays a critical role in the chemical evolution of stellar populations throughout the galaxy's lifetime. The ISM comprises  $\sim 10\text{-}15\%$  of the baryonic mass, including all of the metals in the disc and bulge not otherwise locked up in stars. Circulation of the ISM is also the means by which these metals are transported from their production sites throughout the galaxy, to be incorporated in future stellar generations, with significant opportunity for gas-phase and

dust surface chemical reactions to occur along the way. How this circulation operates, and what happens to the metals throughout the process, will have an impact on the galactic chemical evolution on scales ranging from that of individual star formation sites to the extent of the galactic disc.

Different phases of the ISM — e.g., diffuse atomic gas, dense molecular gas, dust — have been mapped with particular sets of tracers, each providing different types of information. For example, HI emission maps provide the velocity distribution and total column density of HI atoms along the line of sight, but do not

---

\* NSF Postdoctoral Fellow

contain direct information on the distances of the clouds. Emission-based dust maps provide the integrated dust column density (assuming some temperature properties, among others), and extinction-based dust maps can provide the three-dimensional distribution of dust but not the velocities of the clouds. A comprehensive picture of the ISM requires having a complete set of tracers, able to probe all chemically and dynamically relevant components of the ISM, along with an understanding of how these components interact with each other. The Milky Way, and to some extent M31, are the only large galaxies where it is possible to probe not only the three-dimensional distribution of the ISM components, but also to resolve their velocity behavior on small scales, using the distances of individual stars within the galaxies.

One of the ISM components that remains under-explored in the Milky Way is the regime of carbon-rich large molecules — e.g., polycyclic aromatic hydrocarbons (PAHs) and fullerenes. Comprising tens to hundreds of atoms, these molecules comprise an large family of species, with an enormous variety of chemical substitution possibilities, excitation states, and so on. Their presence is detected in absorption signatures in certain dense environments, and in emission (e.g., in mid-IR spectroscopy and imaging) near bright irradiating sources. But it remains largely unknown how these C-rich molecules are distributed away from these particular environments, what form they take in the larger part of the galaxy, and how these properties impact the later stellar generations that form out of that ISM.

Recently, a promising approach has arisen that can trace the signatures of this molecular family, at the same kinds of scales on which we map other ISM components. The diffuse interstellar bands (DIBs) are a set of  $\sim 400$  optical/IR interstellar absorption features that can be detected superimposed on the spectra of stars throughout the Milky Way and extragalactic sources (for an extensive or short review, respectively, see Herbig 1995; Cox 2011). The exact chemical identification of the DIB feature carriers remains an unsolved puzzle, but the current evidence strongly favors multiple species of these large,

C-rich molecules (PAHs, other hydrocarbons, fullerenes), and as such, the DIBs provide a means of tracing this critical but elusive component of the ISM.

However, until relatively recently, the study of DIBs relied largely on small samples ( $N < 100$ s) of spectra of bright, relatively nearby stars. To reach beyond the solar neighborhood, a few groups (Kos et al. 2013; Puspitarini et al. 2015; Zasowski et al. 2015) have developed methods to measure DIB absorption in the spectra of cooler stars — especially in the spectra of luminous giant stars, lying up to several kpc from the Sun. Zasowski et al. (2015) in particular demonstrated the ability to measure a precise mean radial velocity (RV) for the  $1.527\mu\text{m}$  DIB they studied along each line of sight, with the distribution of the DIB carriers themselves constrained by the distribution of the stars in the sample<sup>1</sup>.

In this contribution, we combine these DIB measurements (§2) with three-dimensional dust maps based on the Pan-STARRS survey (§3) in order to demonstrate the feasibility of assigning distances to the C-rich molecules giving rise to the DIB features, or conversely assigning velocities to individual diffuse dust clouds (§4). This is something that has not yet been done with either extinction- or emission-based dust measures. We briefly discuss the implications of this approach in §5 and conclude in §6 with a short summary of how *Gaia* will contribute to this type of effort in the near future.

## 2. DIB measurements

### 2.1. The APOGEE dataset

The spectra used for this study come from the APOGEE project (Majewski 2012), a high-resolution ( $R \sim 22,500$ ), near-IR, multi-object spectroscopic survey operating as part of the Sloan Digital Sky Survey (Eisenstein et al. 2011). The primary targets of APOGEE are

<sup>1</sup> The dataset used in both that paper and this present analysis can be downloaded here: [http://www.pha.jhu.edu/~zasowski/docs/APOGEE\\_DIB\\_Catalog.html](http://www.pha.jhu.edu/~zasowski/docs/APOGEE_DIB_Catalog.html).

red giant stars at heliocentric distances of several kpc, probing not only the halo but also the disc and bulge of the Milky Way. The spectra used here include the publicly released SDSS DR10 dataset, as well as some spectra taken during the second year of the survey, which have now been released as part of DR12<sup>2</sup>. For details of the APOGEE targeting, data reduction, and spectral analysis, see Zasowski et al. (2013), Nidever et al. (2015), and Holtzman et al. (2015), respectively.

## 2.2. The 1.527 $\mu$ m DIB

The majority of well-studied DIBs lie at optical wavelengths. The  $H$ -band feature studied here, at 1.527 $\mu$ m, was first discovered by Geballe et al. (2011). Zasowski et al. (2015) showed that this DIB’s absorption strength is particularly well-correlated with the line-of-sight dust reddening (both integrated to the distance of the background star), and that the mean DIB velocity field resembled that of a rotating disk, with deviations due to kinematical substructures and non-circular rotation within the disk.

The DIB feature was isolated from the background stellar spectrum by using a synthetic spectrum of the appropriate stellar parameters ( $T_{\text{eff}}$ ,  $\log g$ ,  $[\text{Fe}/\text{H}]$ , etc.) to identify and remove the stellar lines. The residual interstellar DIB absorption within the wavelength window of interest was then fitted with a single gaussian curve to measure the feature’s equivalent width  $W_{\text{DIB}}$ , central wavelength  $\lambda$ , and line width  $\sigma$ . The observed central wavelength was then compared to the estimated rest wavelength ( $\lambda_0 = 1.52724\mu\text{m}$ ) to calculate the mean (density-weighted) velocity  $v$  of the carriers along each line of sight. Further details of this DIB extraction and fitting can be found in Zasowski et al. (2015). We restrict our sample to “well-measured” features as defined in §4.1 of that paper, to ensure reliable velocity measurements.

## 3. Dust distribution measurements

Three-dimensional dust mapping is a notoriously difficult task, but one that is critical to exploring not only the ISM but also the stellar populations in the Galaxy, particularly in the dusty disk midplane and bulge (wherein lies most of the stellar mass). In this contribution, we adopt the recent “PS1” dust map of Green et al. (2015), which provides  $E(B - V)$  reddenings over nearly all of the sky with  $\delta > -30^\circ$  (well-matched to the APOGEE footprint). The map pixels range between  $\sim 3'$  and  $\sim 13'$  on a side, and the distance modulus resolution is  $\Delta\mu = 0.5$ . The reddening estimates are based on probabilistic SED fits to  $\sim 800\text{M}$  stellar sources from PanSTARRS and 2MASS; see Green et al. (2015) for more details.

We extracted the cumulative reddening towards each star (§4) to confirm that this integrated reddening follows roughly the same relationship with  $W_{\text{DIB}}$  as measured by Zasowski et al. (2015) using star-by-star color excess-based reddening (i.e., true foreground-only reddening values). These relationships are shown in Figure 1. We find comparable trends, with an increased scatter in the PS1 relationship, especially at high reddening. This is plausibly due to the discrete distance bins of the PS1 reddening, which become quite large at the distances of many of the stars in the APOGEE sample. But overall the mean agreement is very good.

## 4. Towards dust cloud kinematics

To reliably match the velocity measurement (from the 1.527 $\mu$ m DIB) with the distance measurement (from the dust) along a particular line of sight, we would like to ensure that the ISM along that line of sight is dominated by material in a very narrow range of distance. This ensures that the single velocity measured from the DIB feature, which is intrinsically weighted by the carrier density distribution, can be meaningfully assigned to a single mean distance.

For this initial effort, along each midplane line of sight with a DIB  $v$  measurement (with  $|b| < 10^\circ$ ), we (i) calculated the differential red-

<sup>2</sup> <http://www.sdss.org/dr12/>

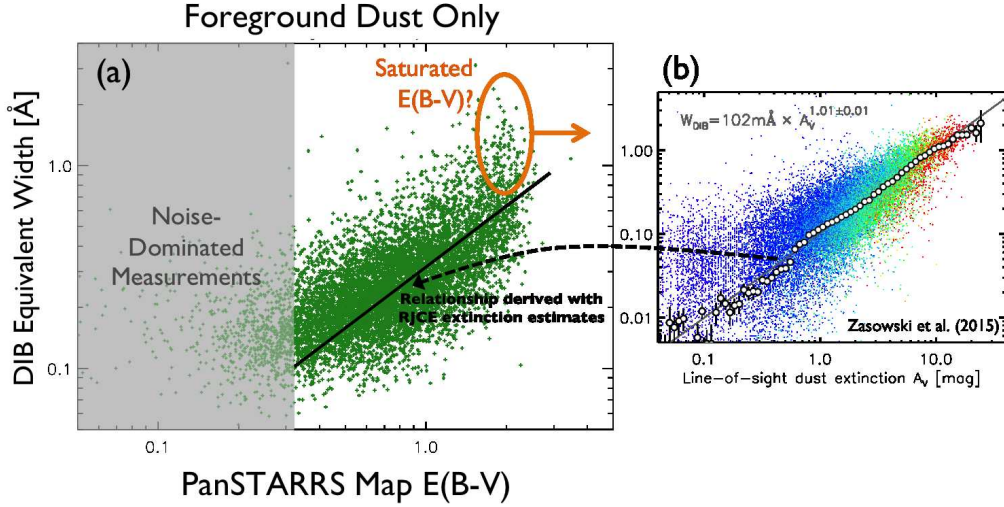


**Fig. 1.** (a): Relationship between DIB equivalent width ( $W_{\text{DIB}}$ ) and cumulative PS1 reddening up to the position of each star. The black line is not a fit to these data, but rather the trend measured between  $W_{\text{DIB}}$  and the total stellar extinction in the right-hand panel, converted to  $E(B-V)$  assuming an  $R_V = 3.1$  extinction law. The orange circle indicates sightlines where the PS1 map is possibly saturated, and the gray box denotes the region where the DIB is likely to be too weak for a confident velocity measurement. (b): Relationship between  $W_{\text{DIB}}$  and  $A(V)$ , measured with the RJCE method (Figure 5 in Zasowski et al. 2015).

dening  $\Delta E(B-V)$  in each distance bin foreground to the star, (ii) measured the mean and dispersion of  $\Delta E(B-V)$ , and (iii) identified the peaks (“clouds”) that rose more than three times the dispersion above the mean. Provided the peaks were not spread widely along the line of sight, we then (iv) weighted their distances by  $\Delta E(B-V)$  and calculated a mean line-of-sight dust distance  $d$ . (We also experimented with using the single strongest reddening peak, with varying the dispersion cut, and so on. The qualitative findings below were unchanged, but this particular procedure produced the smoothest results.)

Figure 2a shows the result of combining the set of cloud distances  $\{d\}$  and cloud velocities  $\{v\}$ . This is a top-down view onto the Galactic disk, with the Sun at  $(X, Y) = (-8, 0)$  kpc, and the Galactic Center (at  $l = 0^\circ$ ) off to the right. The color of each pixel represents the mean RV of the DIB absorbers in the pixel associated with the dust position. The pattern of the rotating Galactic disk is evident.

For comparison, Figure 2b shows the velocity pattern predicted by a Galactic rotation

curve (Clemens 1985) sampled at the  $XY$  positions of the clouds. The pattern is extremely similar, and the residuals between the two (Figure 2c) is both very nearly zero and flat in  $XY$ . This would not happen if the DIB velocities were being assigned to inappropriate distances, or equivalently, if the dust clouds at particular distances were being assigned inappropriate velocities. This confirms that the DIB absorption is correlated with the dust absorption not only in the mean along each line of sight, but also in specific clouds at specific distances.

## 5. Implications

The full phase space of the ISM (e.g., composition, 3-D density  $\rho(\vec{X})$ , 3-D velocity  $V(\vec{X})$ ) remains incompletely characterized, with varying levels of spatial distribution and radial velocity information available for different components (§1). One element that has been almost completely missing is the kinematics of interstellar dust. Prior work focused on measuring

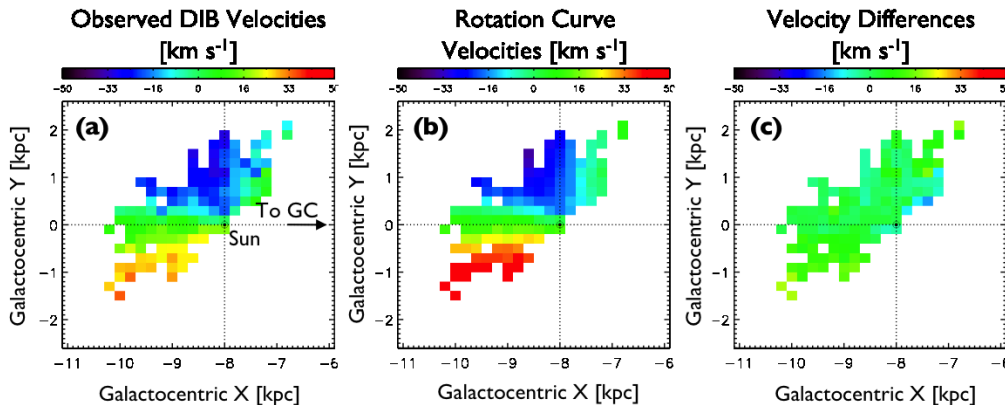


**Fig. 2.** Face-on views of the Galactic disk, with the velocity information of the dust indicated by the color of each pixel. The Sun is at  $(X, Y) = (-8, 0)$  kpc as labeled. (a): Observed radial velocities of the DIBs. (b): Radial velocities of the dust predicted by the rotation curve of Clemens (1985). (c): Difference between the observed and model velocities  $((b) - (a))$ .

the velocities of very dense clouds — via CO emission, for example. Aside from some measurements of very local, solar system dust particles (e.g., May 2008), dust velocities have never been directly measured for dust in diffuse clouds.

Constraining the velocities of these clouds is critical for understanding the circulation of dust throughout the disk, including radial flows alongside metal-rich and metal-poor gas, redistributing heavy elements throughout the Galaxy. Dust expulsion into, or dust accretion from, the thick disk and halo drive the vertical motion of dust clouds (relative to the disk), and the kinetic energy of those processes impacts the quantity of dust in the outermost regions of galaxies (e.g., Ménard & Fukugita 2012) and the injection of heavy elements into star formation sites throughout the disk.

With this new technique, we demonstrate for the first time the ability to measure velocities associated with diffuse dust clouds across several kpc of the Galactic disk (not just those dense enough to host significant quantities of dense gas). This represents a critical new piece of the multi-dimensional ISM puzzle, carrying unique information on both the stellar and interstellar chemical evolution of the Galaxy.

## 6. Looking towards *Gaia*

Though much anticipation is focused on the wealth of *stellar* information that *Gaia* will deliver, there are at least two ways in which *Gaia*'s data will be applicable to the questions described here. The first is that the spectrophotometry from the BP/RP detectors will provide an estimate of the extinction  $A(V)$  — and even the extinction law parameter  $R_V$  — to each star. When combined with the distance estimates to many of those stars, *Gaia* alone will enable a high-quality three-dimensional extinction map, and will provide refinements and corrective scalings to existing maps. The second aspect of *Gaia*'s dataset to anticipate is the measurement of the 8620Å DIB, which lies within the wavelength range of the RVS and can thus be measured for tens of millions of stars, assuming the stellar flux can be modeled correctly. This DIB is also usefully well-correlated with reddening (e.g., Munari 2000). The RVS's spectral resolution of  $\sim 11,500$  is high enough to measure the mean velocities of these features — more coarsely than the higher-resolution APOGEE ones, but over a quantity of stars that will enable a more statistically robust mapping of the 8620Å velocity field throughout several kpc of the Galaxy.

*Acknowledgements.* We are deeply grateful to G. Green and D. Finkbeiner for their assistance in working with the PS1 dust map.

## References

- Clemens, D. P. 1985, *ApJ*, 295, 422  
Cox, N. L. J. 2011, *IAU Symposium*, 280, 162  
Eisenstein, D. J., Weinberg, D. H., Agol, E., et al. 2011, *AJ*, 142, 72  
Geballe, T. R., Najarro, F., et al. 2011, *Nature*, 479, 200  
Green, G. M., Schlafly, E. F., Finkbeiner, D. P., et al. 2015, *ApJ*, 810, 25  
Herbig, G. H. 1995, *ARA&A*, 33, 19  
Holtzman, J. A., Shetrone, M., Johnson, J. A., et al. 2015, [arXiv:1501.04110](https://arxiv.org/abs/1501.04110)  
Kos, J., Zwitter, T., Grebel, E. K., et al. 2013, *ApJ*, 778, 86  
Majewski, S. R. 2012, *American Astronomical Society Meeting Abstracts* #219, 219, #205.06  
May, B. H. 2007, *A Survey of Radial Velocities in the Zodiacal Dust Cloud* (Springer, New York)  
Ménard, B., & Fukugita, M. 2012, *ApJ*, 754, 116  
Munari, U. 2000, in *Molecules in Space and in the Laboratory*, I. Porceddu and S. Aiello eds., *Italian Phys. Soc. Conf. Proc.*, 67, 179  
Nidever, D. L., Holtzman, J. A., Allende Prieto, C., et al. 2015, [arXiv:1501.03742](https://arxiv.org/abs/1501.03742)  
Puspitarini, L., Lallement, R., Babusiaux, C., et al. 2015, *A&A*, 573, A35  
Zasowski, G., Johnson, J. A., Frinchaboy, P. M., et al. 2013, *AJ*, 146, 81  
Zasowski, G., Ménard, B., Bizyaev, D., et al. 2015, *ApJ*, 798, 35